Experimental Setup for Mechanically Testing Subscale Triangular, Rollable, and Collapsible Deployable Composite Booms

Cyrus J. R. Kosztowny*[1][0000-0003-4603-6861], Gregory D. Dean[1], David Long[2], Richard A. Larson[2][0000-0001-8525-3557], Jason P. Moore[1], José E. Morel[1], Joshua E. Salazar[1], Matlock M. Mennu[1], and Nathaniel W. Gardner[1]

[1] NASA Langley Research Center, Hampton, VA 23681, USA
[2] Analytical Mechanical Associates, Inc., Hampton, VA 23681, USA
*Corresponding author
cyrus.j.kosztowny@nasa.gov

Abstract. High-strain composite deployable space structures are used for space infrastructure and science applications such as solar array supports, antennae, camera masts, and lightweight structures supporting solar sailing propulsion elements. Triangular, Rollable, and Collapsible (TRAC) deployable composite booms are one example of a high-strain composite deployable structure and were studied using novel experimental test and characterization methods developed under the Gravity Offloading and Analysis of Long Imperfection-sensitive Elements (GOALIE) project. In the present work, a subscale 7-m-long TRAC boom was suspended vertically to orient gravity along the length of the boom. By orienting vertically, highly nonlinear and unstable behavior often encountered during horizontally oriented gravity offload testing of similar structures was reduced. Pretest analytical predictions of TRAC booms indicated three unique failure modes, loads, and locations for three unique loading cases of in-plane bending, out-of-plane bending, and axial compression. To investigate the predicted behavior, an experimental test was set up to impart mechanical loads to a subscale TRAC boom. The experimental setup, loading cases, and instrumentation used to characterize the mechanical response of a subscale TRAC boom are described in this paper.

Keywords: Deployable Structures, High-Strain Composites, Experimental Testing.

1 Introduction and Motivation

Many space structures such as solar energy collectors, radiators, and observation sensors exhibit improved performance and structural efficiency at scales larger than typically allowable from launch-vehicle payload volume constraints [1]. However, the volume that would be required to put large-scale conventionally assembled structures in orbit is extremely costly. Additionally, large-scale conventionally assembled structures often require difficult in-space assembly operations and possibly multiple launches

depending on the final object size. A payload must be contained within the volume of the payload fairing atop a rocket launch vehicle, and for final structures larger than that volume, multiple launches would be required to get all elements to orbit followed by assembly in space. As a possible solution to volume and mass constraints in payload fairings, high-strain composite structures are extremely lightweight, able to be rolled and stowed into a compact volume for launch and deployable on orbit. High-strain composite deployable structures have been used for various space applications such as solar array supports [2, 3], antennae, instrument masts, and booms supporting solar sail membranes [4]. Lightweight, large-scale, yet stowable structures enable novel spacecraft concepts, such as solar sails, which can expand to become many times larger than their stowed configuration.

Solar Cruiser is one such future spacecraft and would be the largest solar sailing demonstrator NASA has flown [4]. Solar Cruiser is comprised of four triangular sail quadrants supported by four 30-m-long TRAC booms that are deployed from a central hub as shown in Fig. 1.

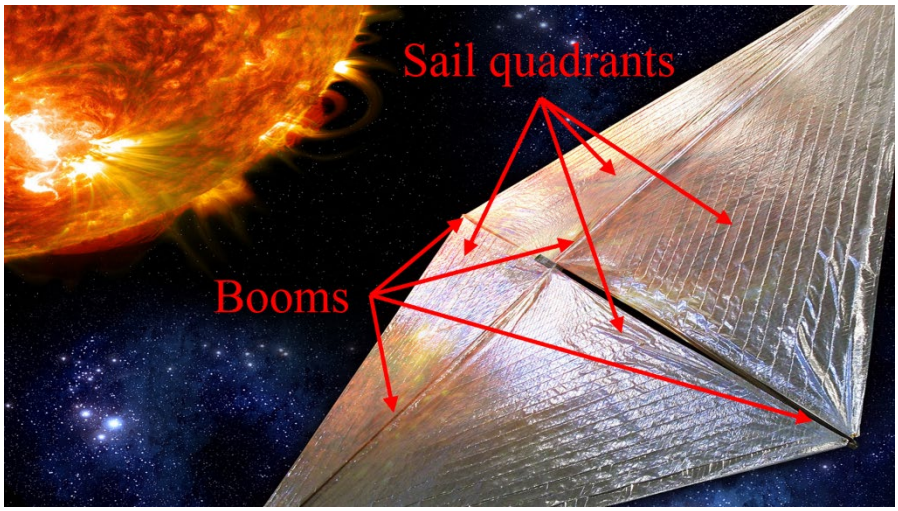

Fig. 1. Artistic rendition of Solar Cruiser with four booms supporting four sail quadrants.

Part of spacecraft development, Technology Readiness Level 6, specifically, requires demonstration of systems in flight-like environments. For the structural sail system on Solar Cruiser, “flight-like” could be interpreted to mean vacuum and microgravity environments. Testing a 30-m-long boom in microgravity yet still on Earth is not feasible. While lightweight, the TRAC boom is sensitive to the effects of gravity because it is compliant in transverse and torsional directions. Because Earth’s gravity cannot be avoided for a ground-based test, gravity offloading methods must be used. Previous attempts at gravity offloading, including methods such as wiffletrees, were implemented for structural testing of TRAC booms [5]. However, the wiffletree mechanisms constraining the boom impart shape changes and restrict select degrees of freedom. Also, geometric features such as twist and local cross-section shape variation may

not be observed when horizontally offloaded because gravity tended to untwist TRAC booms and homogenize the cross-section shape when oriented in a horizontal configuration. Other methods such as microgravity flight tests on aircraft have been conducted in an attempt to capture offloaded performance [6].

To provide an alternate testing configuration than horizontal offloading, a subscale TRAC boom was vertically suspended to align the stiffest direction of the structure with gravity. By testing in a vertical orientation, destabilizing loads often observed during the collapse of the cross section of the TRAC boom could be avoided, though the response of TRAC booms was anticipated to be dominated by highly nonlinear shell-like mechanisms like buckling and instabilities [7]. In the GOALIE project, experimental mechanical test methods were developed in conjunction with finite element analysis (FEA) models. The models included accounting for gravity and twist [8] for booms ranging from 2 m up to 30 m in length, and therefore longer than what had previously been demonstrated in a vertical orientation [9]. The numerical modeling approach may be validated with experimentally collected test data by using the setup described in this paper. With validated analysis models, FEA modeling of TRAC booms under microgravity environments may have increased confidence of their accuracy.

The test approach and setup for a 7-m TRAC boom is described in the next section. Multiple instrumentation systems were implemented for the subscale test and are discussed in Section 3. Lastly, concluding remarks are provided in Section 4.

2 Test Approach and Setup

The quasi-static mechanical subscale testing had two intended purposes. The first purpose was to demonstrate experimental testing capability while developing experience working with long, slender, and flexible structures in preparation for the full-scale (30-m-long TRAC boom) test. The second purpose was to collect test data for analysis model validation. With respect to the second purpose, strong dependence on loading direction was observed in analysis of the test article as discussed in Ref. [8]. As the test was designed to provide a dataset to be used for analysis model validation, the analysis results were used to inform the test setup on what type of data should be collected and where along the test article the data should be collected from. The experimental test setup was for quasi-static mechanical loading of a fully deployed subscale carbon fiber composite TRAC boom in ambient conditions. The nominal cross-section of the TRAC boom is shown in Fig. 2 with parameters of the cross-section provided in Table 1.

The test article was installed in a vertical orientation with fixed and free conditions at the root and distal ends, respectively. Distal-end mechanical loading was set up for the subscale test article. Three load cases were considered for the subscale test: out-of-plane bending, in-plane bending, and off-axis compression. The in- and out-of-plane bending was with respect to the solar sail membrane plane that could exist in a solar-sailing structural system, and the loading directions relative to the distal end of the test article are shown in Fig. 3.

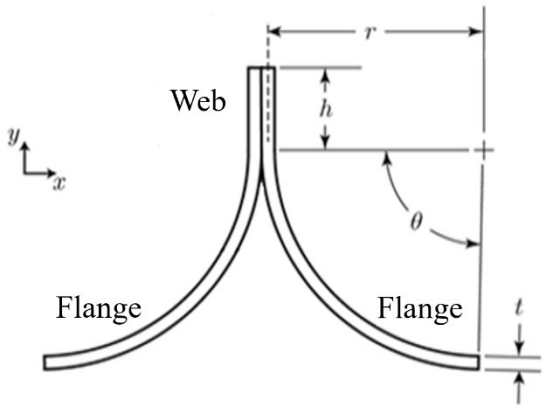

Fig. 2. Nominal cross-section schematic of the TRAC boom test article.

Table 1. Nominal TRAC boom cross-section parameters.

Parameter	**Value**
Flattened height	0.127 m
Flange radius, *r*	0.0782 m
Web height, *h*	0.017 m
Laminate thickness, *t*	0.252 mm
Flange sweep angle, θ	80.9 degrees

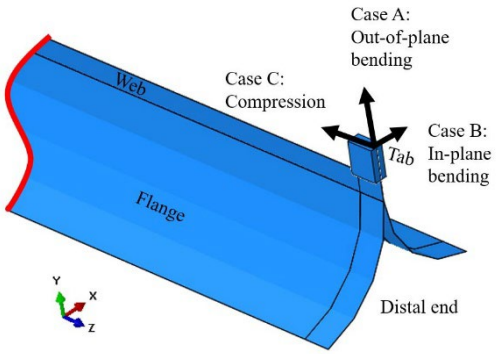

Fig. 3. Three mechanical loading directions considered for subscale testing.

2.1 Facility

The test facility, called the Thor tower, is a 4.1-m-wide by 6.1-m-long by 31.6-m-tall enclosed tower as shown in Fig. 4 with four elevated platforms. The platforms at levels 4, 7, 10, and 12 are 7.7-m, 15.2-m, 22.8-m, and 27.8-m above the ground, respectively. Each platform contains a centrally located opening that facilitates suspending a continuous structure from the ceiling of the tower to the floor. The Thor tower is part of the

Structural Dynamics Branch facility in Building 1293B at NASA Langley Research Center. In the first five levels of the tower, there are two large, steel backstops providing rigid reaction walls. The subscale test activity involved operations only from the first platform (level 4) to the ground because the subscale test article was 7 m long.

2.2 Hardware

Hardware was designed and installed to perform three primary functions:

1. To constrain the test article in a vertical orientation while providing for ease-of-access and operations via the test article fixture.
2. To locate and support all test instrumentation equipment throughout the test activity for successful data collection.
3. To react displacement-controlled loading forces through an adjustable frame.

An overview of the subscale test hardware setup is shown in Fig. 5. The fixture, instrumentation supports, and Vention[1] frame for load introduction are discussed in the following subsections.

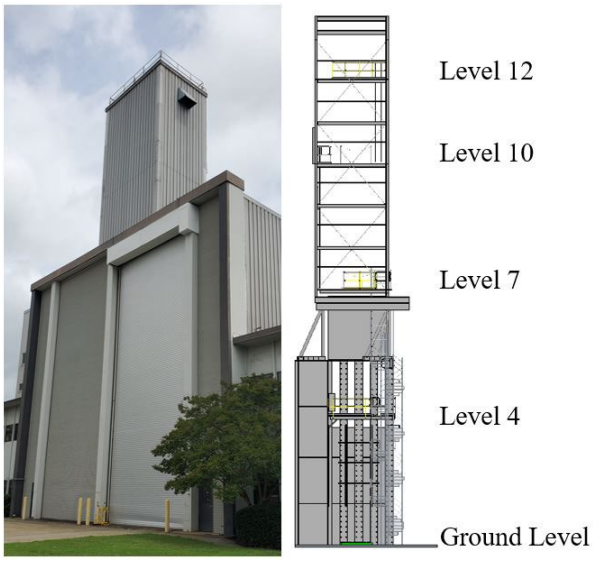

Fig. 4. Thor tower (left) and CAD representation (right).

Fixture. The primary purpose of the test fixture was to restrain the root-end of the test article during mechanical loading. The fixture was comprised of a beam spanning the opening at the 4th platform, two attachment legs at each end of the beam, and the root-

[1] The use of trademarks or names of manufacturers in this report is for accurate reporting and does not constitute an official endorsement, either expressed or implied, of such products or manufacturers by the National Aeronautics and Space Administration.

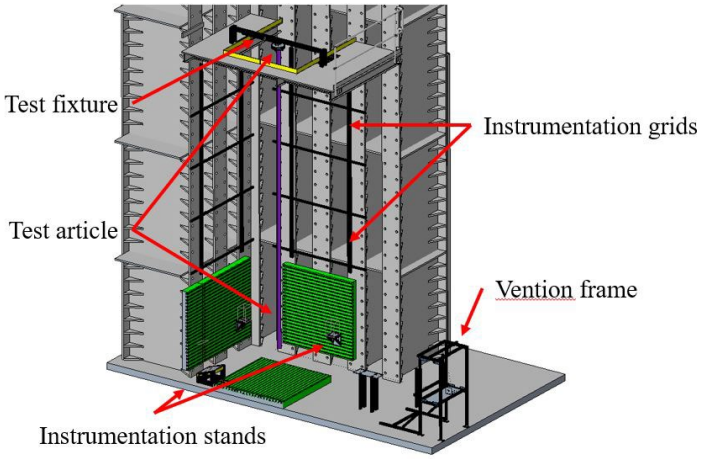

Fig. 5. Subscale test hardware and facility overview.

end restraint assembly as shown in Fig. 6. Details of the root end assembly are shown in Fig. 7. The root-end restraint assembly was comprised of a circular metal plate and a three-dimensional (3D) printed clamp that maintained the open, unloaded cross-sectional geometry of the test article and fastened to the circular metal lower rotation plate. Additional components of the root-end restraint assembly included an upper rotation plate, and a set of leveling bolts. The upper rotation plate enabled recording rotation about the long-axis of the test article as it was oriented for each loading configuration. The leveling bolts rotated the lower rotation plate about both axes perpendicular to the test article to enable leveling of the boom to be in-line with gravity. The installed test article is shown in Fig. 8.

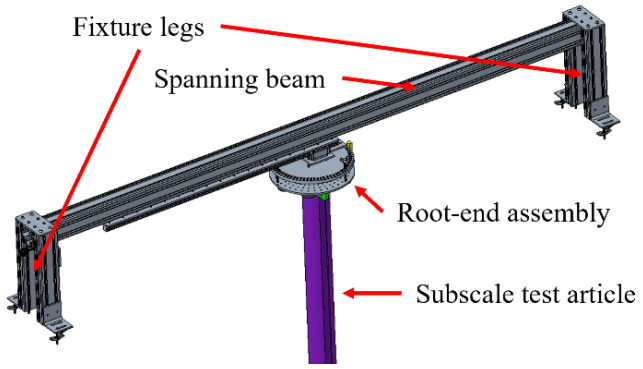

Fig. 6. Subscale test fixture with test article.

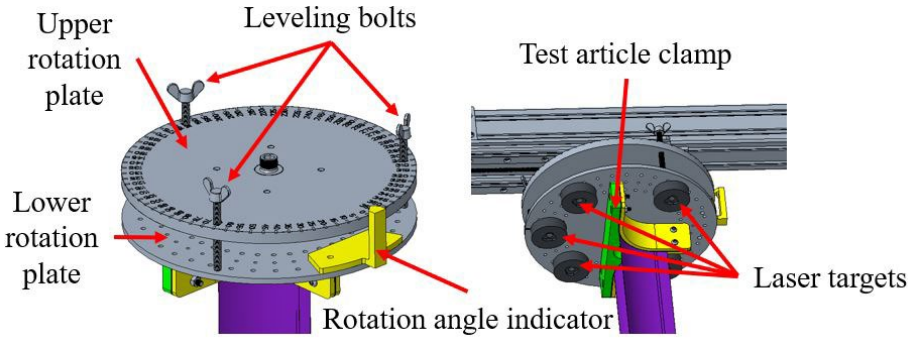

Fig. 7. Root end assembly details.

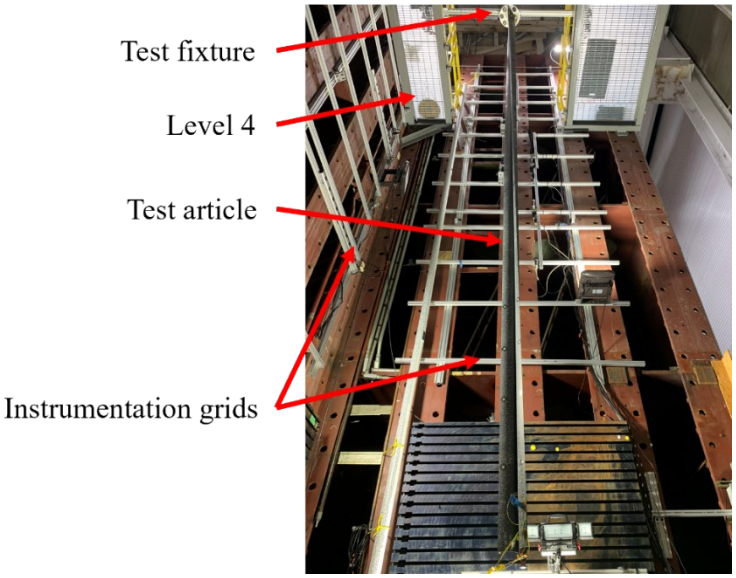

Fig. 8. Test article installed in the test facility.

Instrumentation Support. Multiple supports were created so instrumentation could be secured in a position that enabled high-quality data collection and verification of the test article and test hardware. Two grids were constructed of aluminum T-slot extrusion and secured to the face of the backstops in the test facility. Each grid consisted of two vertical members to which horizontal members were fastened. The vertical position of each horizontal member was designed to be adjustable so that instruments were positioned in the best location to collect high-quality data. Two other types of mounts were created to support laser tracking equipment. One was a base for a FARO Vantage laser tracker that was placed adjacent to the test article to inspect the root-end fixture for possible movement during testing. The other were two mounts for securing two Leica Total Station 15 (TS15) theodolites to the backstops to record the distal-end displacement of the test article during testing.

Load Introduction. Loading was designed to be performed by an electrical motor winding a cable (i.e., prescribed line shortening) that was redirected with a set of pulleys to impart the desired distal-end deflection for each loading configuration. Motor and pulleys were placed on a purpose-built Vention frame designed to react the loads imparted upon the test article as shown in Fig. 9.

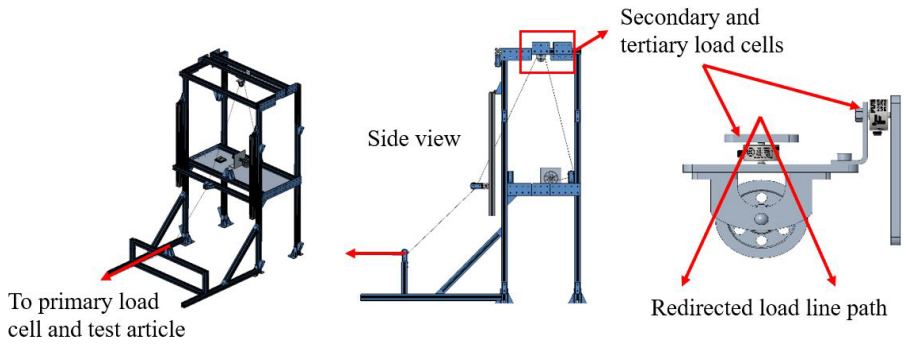

Fig. 9. Vention frame and load cell locations.

A cable was connected to the distal end of the test article by a 3D-printed tab. The tab also secured a prism that was used to track distal end position by a laser tracking system that is discussed in a later section. For the off-axis loading configuration, the cable was routed through a pulley fastened to the spanning beam of the test fixture before being routed through the pulleys on the Vention frame as shown in the comparison of load line routing in Fig. 10.

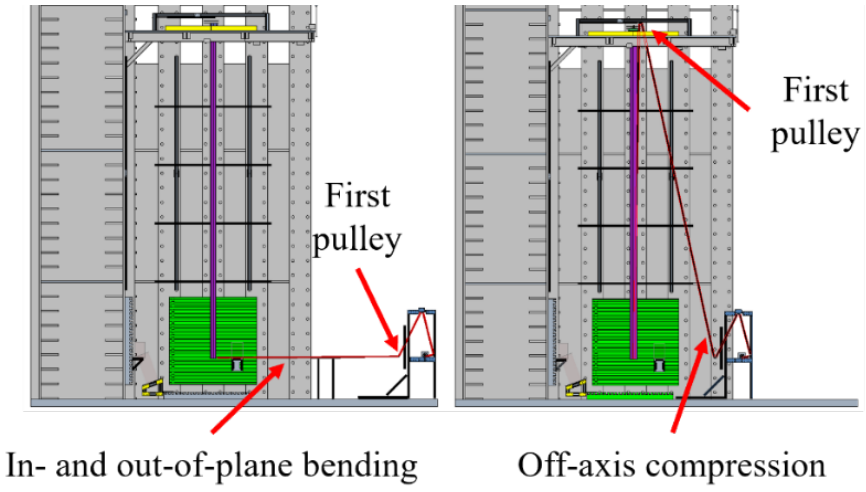

Fig. 10. Load-line routing comparison.

The distance from the root to the pulley on the spanning beam resulted in an approximate 1-degree offset from the axis of the test article. The offset was representative of

the intentional offset designed into the Solar Cruiser sail system where one degree was the smallest offset that could be achieved due to hardware constraints. The offset as implemented was intentional so that the off-axis loading condition anticipated during flight could be included as part of the validation dataset. A summary of the predicted maximum anticipated loads from Ref. [8], including effects of twist and gravity, and the number of pulleys used for each load case are provided in Table 2. A minimum of three pulleys were necessary to ensure the load line would be taken up by the spool in a consistent direction regardless of the loading case. The fourth pulley, included for the off-axis compression case, was implemented to enable the load-line redirection capability.

Table 2. Load case peak loads and load-line redirections with pulleys.

Load Case	Peak Load (N)	Pulley Count
A	8.9	3
B	2.2	3
C	79	4

3 Instrumentation and Representative Data

The subscale test campaign is to serve, in part, as a demonstration of the capabilities and limitations of test instrumentation systems to determine which systems are applicable for the full-scale test. Much of the instrumentation may be considered redundant in the type of data that was collected (e.g. displacement and strain data), however, the locations of instrumentation were dictated by the predicted response from analysis from Ref. [8]. Locations of potential collapse and high-strain regions were instrumented using a combination of non-contacting and contacting instrumentation systems. Non-contacting instrumentation systems were preferred as these systems typically impart the least shape-changing influence on the test article compared to contact-based instrumentation systems. A 0.1 Hz external triangle wave was selected to synchronize data recorded by the fiber optic, digital image correlation, load, and motor encoder data acquisition systems as a function of time to ensure correlation. A summary of the types of data each system was set up to collect for correlation is provided in Table 3. The test instrumentation systems set up for subscale testing are described in the following subsections.

3.1 Motor Displacement

The as-applied displacement was designed to be collected from an encoder as part of the electrical motor that served as the actuation device. The motor was designed to operate in displacement control. The difference between the commanded displacement and the observed displacement was implemented as one metric for test control and potential deviation. The motor was the only device designed to be controlled during testing that imparted load to the test article.

Table 3. Type of data anticipated from each instrumentation system.

Instrumentation System	Displacement or Position	Strain	Shape	Load
Load Cells				✓
Motor Encoder	✓			
Digital Image Correlation	✓	✓	✓	
High-Speed Video/High-Speed Digital Image Correlation	No/✓	No/✓		
Fiber Optic Strain Sensing		✓		
Laser Tracker	✓			
Laser Scanner	✓		✓	

3.2 Load

Three load cells were placed to collect reaction loads during load application. The locations of the load cells as shown in Fig. 9 did not change between loading configurations, but the loading configuration influenced the maximum load cell capacity needed for each configuration. An in-line load cell was considered the primary load cell and was installed between the distal-end connection tab on the test article and the first pulley. The first pulley location depended on the load case and is shown in Fig. 10. The secondary load cell was installed on the Vention frame to provide data that may be used to determine line-loss due to friction in the pulleys. The tertiary load cell was installed to the Vention frame and connected to a bracket that secured the secondary load cell to the Vention frame to provide data to indicate if misaligned loads were being applied to the second load cell. The locations of the secondary and tertiary load cells are shown in Fig. 9. All load cells were manufactured by Futek. Load cells with capacities of 4.4 N, 44 N, and 222 N were selected because the three loading cases considered for testing exhibited a range of anticipated loads from 2.22 N for the in-plane bending case to 79 N for the off-axis compression case. The 4.4 N and 44 N load cells were miniature S-beam Jr. type and model LRM200. The 222N load cells were tension/compression in-line type and model LCM300. Loads at the tertiary location were expected to be small compared to the loads applied to the test article because the load line routing path was designed to minimize loads in the direction measured by the tertiary load cell. Details of the load cases, and load cells planned for each case, are provided in Table 4.

Table 4. Predicted maximum load and load cell capacities for each loading case.

Load Case	Maximum Load (N)	Primary Load Cell (N)	Secondary Load Cell (N)	Tertiary Load Cell (N)
A	8.9	40	40	4.4
B	2.2	4.4	40	4.4
C	79	222	222	4.4

3.3 Digital Image Correlation

Digital image correlation (DIC) is a stereoscopic photogrammetric method that employs image registration and tracking techniques to measure full-field displacement and strains. DIC camera pairs, often referred to as a system, were placed along the length of the test article starting at the root and progressing towards the distal end. A total of five low-speed DIC systems were implemented for the subscale test, and approximately 65% of the test article length was within view of the systems. Four DIC systems were located adjacent to one another beginning at the root-end of the test article, and the fifth system was located at the distal end. The four DIC systems located at and adjacent to the root are shown in Fig. 11. Two DIC systems comprised of 12-megapixel (MP) Basler cameras with 16-mm Kowa lenses viewed the test article at and adjacent to the root, while the other three DIC systems were comprised of 6 MP Basler cameras with 8.5-mm Kowa lenses and viewed the central portion of the test article and the distal end. The 12 MP DIC systems had higher effective resolution (pixels per mm) than the 6 MP DIC systems. The 12 MP DIC systems were installed at the root because full-field strains near the root are of interest and the higher effective resolution increased confidence that accurate strain fields were calculated. Strains near the root are of interest because the predicted failure location for the in-plane and out-of-plane loading configurations are within the first 0.5 m from the root of the test article.

Displacement and Strain Fields. An example of a calculated displacement field is shown in Fig. 12 as collected and processed from one DIC system during system checkout. Full-field data was also processed for strain as part of checkout. Both displacement and strain fields can be used to compare the recorded response of the test article with the predicted response from analysis as part of test-analysis correlation.

Test Article Shape from DIC. Combining multiple DIC systems was performed in the postprocessing software, VIC, to stitch images together resulting in 3D data of the as-installed test article shape. Surfaces were extracted from the shape data and can inform twist approximation used in the pretest analysis. Extracted shape or twist may also be implemented as post-test analysis correlation effort. An example of the stitched 3D shape capture data from the DIC systems is shown in Fig. 13.

High-Speed Video and DIC. Two Phantom high-speed digital cameras were placed to record structural collapse of the TRAC boom under mechanical loading. Due to uncertainty where the predicted collapse would form for the in-plane and out-of-plane bending configurations, the cameras were set up for standard video collection mode so that a longer region of the test article root was in the field of view. The high-speed camera setup was designed to be relocated and installed in a stereoscopic configuration for DIC capture for the off-axis compression load case. The collapse mechanism for the off-axis compression case was repeatedly predicted as cross-section flattening and then bending response at the distal end of the test article.

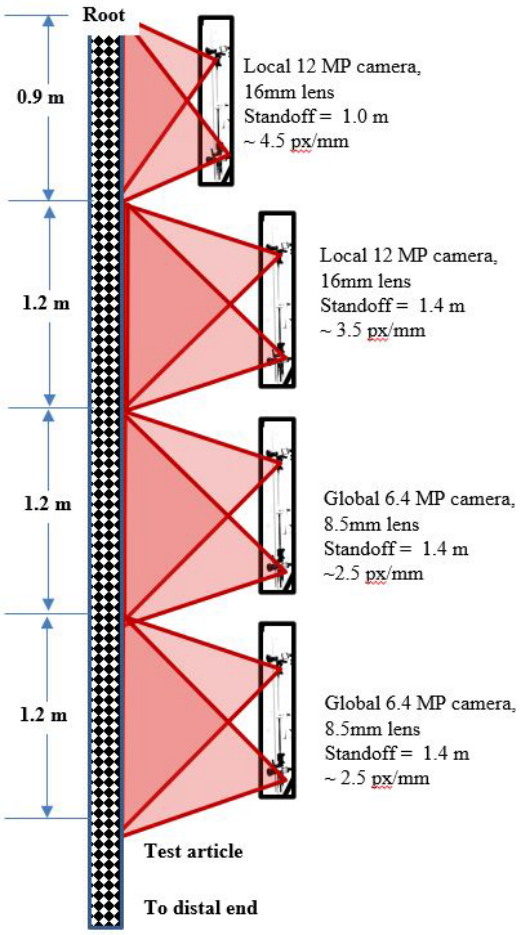

Fig. 11. DIC systems with field of view at the root and root-adjacent stations.

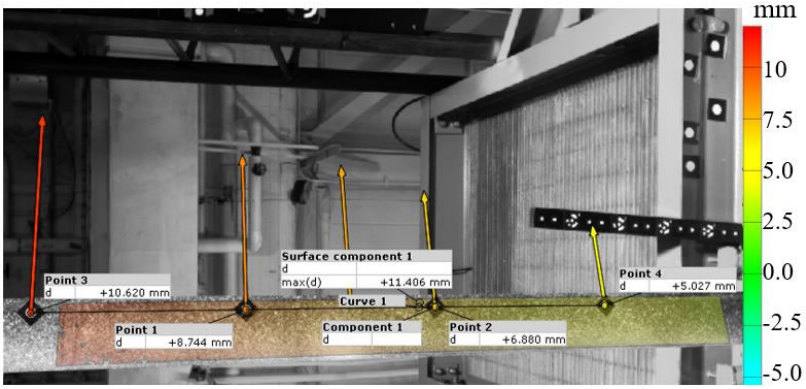

Fig. 12. Example displacement field data from one DIC system image.

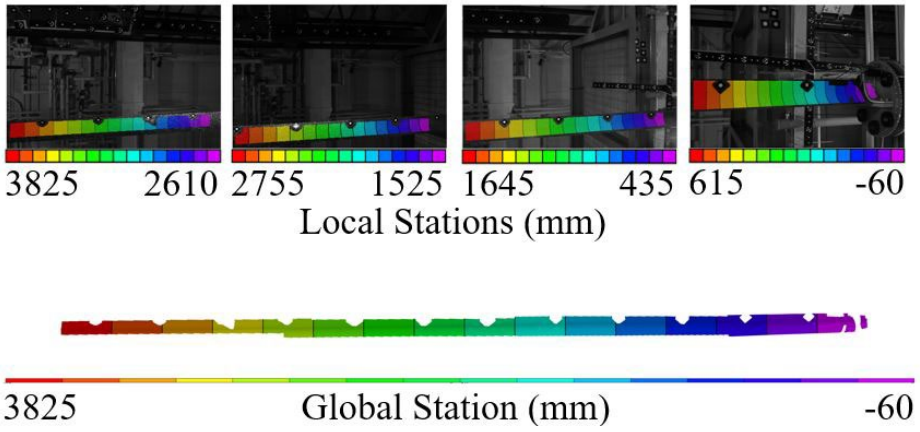

Fig. 13. Stitched DIC images from root (right) to beyond mid-length (left).

Variable focal-length lenses were installed on the high-speed cameras. A field of view of 1 m per camera along the length of the test article was obtained for the bending load configurations, and a field of view of 0.8 m was expected at the distal end. The smaller field of view is due to implementing DIC for the off-axis compression configuration.

3.4 Fiber Optic Strain Sensing

Fiber optic strain sensing (FOSS) uses optical light transmitted and received through optical fibers to measure strain. The technique differs from traditional electrical strain gauges because light is used instead of electricity, and the fibers enable long, one-dimensional strain data collection instead of single point-wise strain collection. FOSS was implemented on the subscale test article because of the uncertainty of the failure location for the in-plane and out-of-plane loading configurations. Strain capture is highly desired at potential failure locations, and FOSS was applied to both flanges and the web for the initial 3 m from the root and again for 0.8 m from the distal end because of the predicted collapse mechanism locations near the root and at the distal end for load cases A/B and C, respectively. FOSS was designed to serve as verification of calculated strain data collected by the DIC systems, and there was high overlap between DIC systems and the FOSS placement. Both longitudinal and transverse strains were designed to be captured with FOSS due to the pattern that was used to lay the fiber.

3.5 Laser-based Scans and Tracking

Surface-based and point-based laser systems were designed and installed to collect both test article data and test facility data during each test. A surface-based laser scanner was installed to collect shape data about the test article. In addition to surface-based scans, point-based measurements on the test article and on the test fixture using laser trackers were installed. The laser tracker target locations were selected so the data may be used

to verify displacement recorded by the DIC systems and to provide data about the test fixture to indicate if undesirable movement occurred during a test.

Test Article Shape from Laser Scans. A FARO Focus S70 laser scanner was installed to collect shape data from the unloaded and loaded configurations of the test article. The Focus laser scanner was placed within the test facility backstop at the mid-length of the test article to maximize the quality of the scan data. Previous observations during a trial scan indicated that the data quality was reduced at the ends of the test article due to long scanning distances. For example, if the Focus scanner were placed in-line with the distal end of the test article, the root-end data was typically of lesser quality than the distal-end data. Therefore, placing the Focus scanner at the mid-length resulted in the best-quality scans compared to other locations. The Focus scanner collected on average 80,000 data points of position per scan from the surface of the test article when installed at the mid-length location. The resulting dataset, often referred to as a point cloud, was collected with the intent to be used as shape verification for shape calculated from DIC-based methods. Purpose-written scripts can also use the point cloud dataset to implement as-installed geometry into finite element analysis models to increase agreement between the as-modeled structure and the as-tested structure. A scan of the subscale test article that was taken prior to test setup completion is shown in Fig. 14.

Fig. 14. Point cloud from scanned subscale test article surface.

Displacements from Laser Trackers. A single Mini-360° prism was secured to the distal end of the test article so that a laser tracker could record distal end location throughout each test. Two Leica Total Station 15 (TS15) theodolites were installed to track the distal end prism. Using two TS15s networked together and inspecting at perpendicular directions relative to each other significantly reduced the uncertainty in the location measurement. A FARO Vantage laser tracker was installed to record the motion of the test fixture during a test. The design of the Vantage system, as implemented, was tailored to collect data that may verify the performance of the test fixture. Analysis results of the test fixture motion indicated the possibility of small, less than 2 mm, deflection under the maximum predicted failure load for the off-axis loading configuration. To understand the performance of the test fixture and to increase confidence that the fixture was performing within requirements, multiple laser targets were secured to the lower rotation plate near the root end of the test article as shown in Fig. 7. At least four targets were visible to the scanner for each loading configuration during test checkout. The target placement was designed to verify whether the test fixture deformed and/or rotated during a test. An example of a trial of the Vantage laser scan data, collected over an hour during test checkout, is shown in Fig. 15.

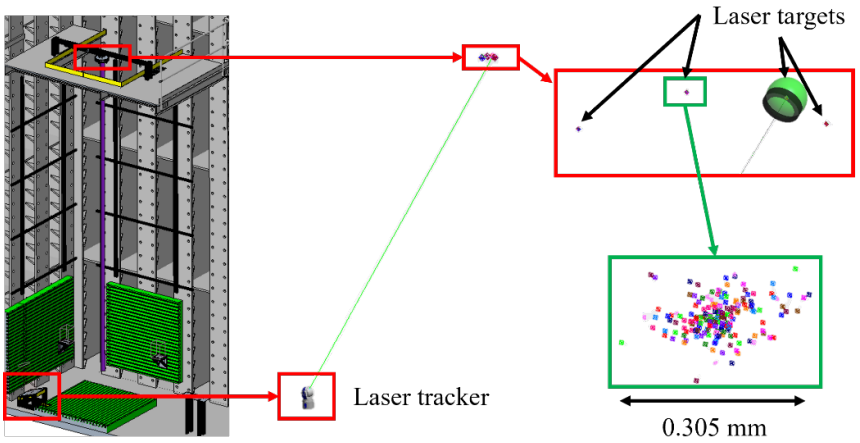

Fig. 15. Laser tracker data collected from the root-end assembly.

4 Concluding Remarks

Experimental test and characterization methods have been developed under the GOALIE project to investigate TRAC deployable composite booms. A 7-m TRAC test article was suspended vertically to orient gravity along the length of the boom thereby reducing highly nonlinear and unstable behavior often encountered during horizontally oriented gravity offload testing. Pretest analytical predictions indicated three unique failure modes, loads, and locations for the three planned loading scenarios. To successfully load to failure and capture all three unique failure mechanisms, numerous test instrumentation systems were implemented for the test. Data from low-speed DIC, high-speed video (and high-speed DIC for one of the three loading configurations), FOSS, laser-surface scanners, laser-target scanners, multiple load cells, and motor encoders were intended to support characterization of the subscale 7-m long TRAC boom test article under in-plane bending, out-of-plane bending, and off-axis axial compression. The test facility and hardware purpose-built to test the response of the subscale 7-m long TRAC boom test article under in-plane bending, out-of-plane bending, and off-axis axial compression were also described.

References

1. Heard, W.L., Bush, H.G., Walz, J.E., Rehder, J.J.: Structural sizing considerations for large space platforms. J. Spacecr. Rockets, 18, 556–564 (1981). https://doi.org/10.2514/3.57852
2. Double Asteroid Redirection Test (DART) Mission Homepage, https://science.nasa.gov/planetary-defense-dart/, last accessed 2024/07/07.
3. Schwanbeck IV, E.R.: Developing Exploration Technologies on the International Space Station (ISS). In: ASE XXXII Planetary Congress,

Houston, TX (2019).
4. Johnson, L., Diaz, C., McNutt, L., Tyler, D., Wallace, D., Wilson, J.: The NASA Solar Cruiser Solar Sail System - Ready for Heliophysics and Deep Space Missions. In: 6th International Symposium on Space Sailing, New York, NY (2023).
5. Nguyen, L., Medina, K., McConnel, Z., Lake, M.S.: Solar Cruiser TRAC boom development. In: AIAA SciTech 2023 Forum, National Harbor, MD (2023). https://doi.org/10.2514/6.2023-1507
6. Richter, M., Straubel, M., Zander, M.E., Salazar, J.E., Chamberlain, M.K., Fernandez, J.M.: Force Application of a Single Boom for a 500-m^2 -Class Solar Sail. In: AIAA SciTech 2023 Forum, National Harbor, MD (2023). https://doi.org/10.2514/6.2023-0938
7. Royer, F., Hutchinson, J.W., Pellegrino, S.: Probing the Stability of Thin-shell Space Structures under Bending. Int. J. Solids Struct. 257, (2022). https://doi.org/10.1016/j.ijsolstr.2022.111806
8. Larson, R.A., Kosztowny, C.J.R., Waters, W.A., Long, D.: Analysis of Triangular, Rollable, and Collapsible Composite Booms under the Effects of Gravity and Twist. In: American Society for Composites 39th Technical Conference, Long Beach, CA (2024).
9. Stohlman, O.R., Zander, M.E., Fernandez, J.M.: Characterization and Modeling of Large Collapsible Tubular Mast Booms. In: AIAA Scitech 2021 Forum, VIRTUAL EVENT (2021). https://doi.org/10.2514/6.2021-0903